Department of Pharmacy[1], Department of Pediatrics[2], The First College of Clinical Medical Science, China Three Gorges University & Yichang Central People's Hospital, Yichang; Beijing Key Laboratory of Active Substance Discovery and Druggability Evaluation[3], Institute of Materia Medica, Chinese Academy of Medical Sciences & Peking Union Medical College, Beijing, P. R. China

Design, synthesis, and biological evaluation of isoquinolin-1(2*H*)-one derivates as tankyrase-1/2 inhibitors

Haiping Yao[1,3], Yanyan Wang[1], Jiangwen Mo[1], Yan Peng[1], Zhu Wang[2,*]

Received November 9, 2020, accepted January 21, 2021

**Corresponding author: Zhu Wang, Department of Pediatrics, The First College of Clinical Medical Science, China Three Gorges University & Yichang Central People's Hospital, Yichang 443003, P. R. China*
wangzhu210@126.com

Pharmazie 76: 132-137 (2021) *doi: 10.1691/ph.2021.0904*

To investigate structure-activity relationships of tankyrase (TNKS) inhibitors, twelve new derivatives of isoquinolin-1(2*H*)-one were designed and synthesized, and biological assessments were conducted. Several potent TNKS inhibitors with single- or double-digit nanomolar IC_{50} values were identified using enzymatic assays. Compound **11c** was the most potent compound of this series and inhibited TNKS1 and TNKS2 at an IC_{50} of 0.009 and 0.003 μM, respectively, and showed an IC_{50} of 0.029 μM in a DLD-1 SuperTopFlash assay. Molecular docking results showed that compound **11c** occupied a unique subpocket and formed a hydrogen bond with Glu1138 of TNKS2, which was not consistent with the patterns of known TNKS inhibitors and thus warrants further research.

1. Introduction

Tankyrase (TNKS)1 (PARP-5a) and TNKS2 (PARP-5b) are important members of the poly ADP-ribose polymerase (PARP) superfamily which share a catalytic PARP domain, transfer ADP-ribose units from their natural substrate NAD^+, and produce poly-(ADP-ribose) polymers on target proteins, resulting in post-translational modification termed poly-ADP ribosylation (also termed PARsylation) (Narwal et al. 2012; Seimiya et al. 2005). TNKS1 and TNKS2 share high sequence and structural homology and common functions, which is pivotal for maintaining the dynamic Wnt signaling pathway via axin PARsylation and regulating telomere homeostasis by modifying the telomere repeat binding factor 1 (TRF1) which is a negative regulator of telomere length (Riffell et al. 2012). Inhibition of TNKS can disrupt the Wnt signaling pathway by stabilizing axin, promoting β-catenin phosphorylation and degradation, and ultimately blocking the expression of oncogenes; moreover, inhibition of TNKS can directly inhibit telomerase activity and thereby impede the extension of chromosome ends, thus preventing cell proliferation (Croy et al. 2016; Sonnenblick et al. 2015). Therefore, TNKS inhibition is hypothesized to be a novel, promising strategy for treating cancer.

Numerous structurally diverse TNKS small-molecule inhibitors have been identified previously; however, TNKS inhibitors are currently not available on the market (Ferri et al. 2017). Based on previous crystallographic studies, TNKS inhibitors can be roughly classified into three categories. The first category comprises nicotinamide mimetic inhibitors (e.g., compound **1** in Fig. 1) which partially mimic the structure of the binding motif of NAD^+, thereby exploiting conserved hydrogen bonds with Gly1032 (TNKS2 numbering) and/or Ser1068 (TNKS2 numbering) in the TNKS nicotinamide binding cavity, similar to the binding features observed in PARP-1 inhibitor complexes (Shultz et al. 2013). The second category includes adenosine binding site-restricted inhibitors (e.g. compound **2** in Fig. 1) which do not share these characteristics of anchoring in the nicotinamide pocket but instead occupy an accessory pocket and interact with the D-loop, and these compounds typically show higher selectivity for TNKS than for PARP-1 and -2 (Bregman et al. 2013). The third category comprises dual binders (e.g., compound **3** in Fig. 1) which occupy both the nicotinamide-binding site and the adenosine-binding site (Haikarainen et al. 2013a, b).

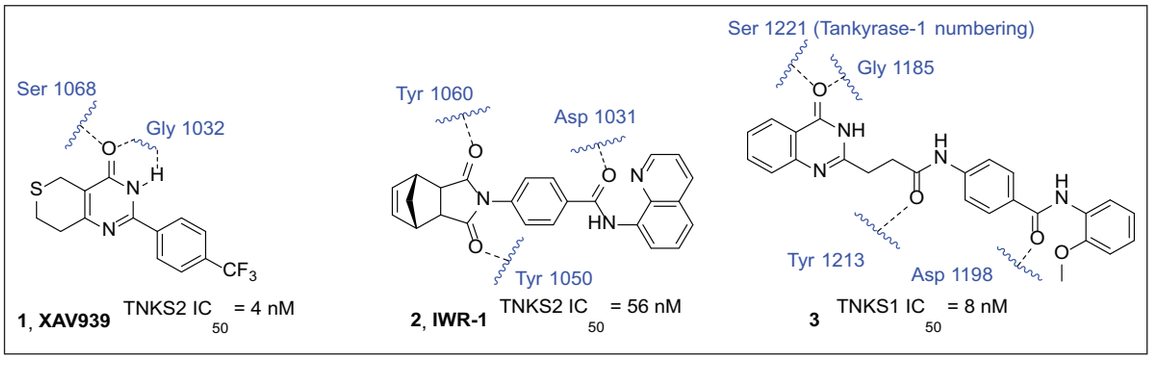

Fig. 1: Binding characteristics of known TNKS1/2 inhibitors and TNKS1/2

As a continuation of our research on design and synthesis of novel inhibitors of PARP family members, we recently focused on the identification of novel TNKS inhibitors (Yao et al. 2015, 2014; Zhou et al. 2018). Based on the characteristics of the catalytic domain of TNKS and on our previous observations of similar scaffolds which act as TNKS inhibitors, a series of isoquinolin-1(2*H*)-one derivatives containing substituent groups at the C-5 position were designed and investigated (Ferri et al. 2017). An isoquinolin-1(2*H*)-one skeleton was constructed to produce the typical hydrogen bonds and π-π stacking interactions with the corresponding amino acids in the nicotinamide binding site of TNKS, which mimics the binding mode of nicotinamide and is an important driver of TNKS inhibition. In order to take advantage of the adenosine binding site, substituents were introduced at the C-5 position, which were expected to be projected into the distal tunnel and to further improve binding affinity. Moreover, an amide group between the isoquinolin-1(2*H*)-one skeleton and the substituents may serve as a linker and improve flexibility and hydrophilicity of the molecules. We here describe the chemical synthesis of novel isoquinolin-1(2*H*)-one derivatives in detail and present TNKS inhibitory activities of these compounds in addition to structure-activity relationship analyses.

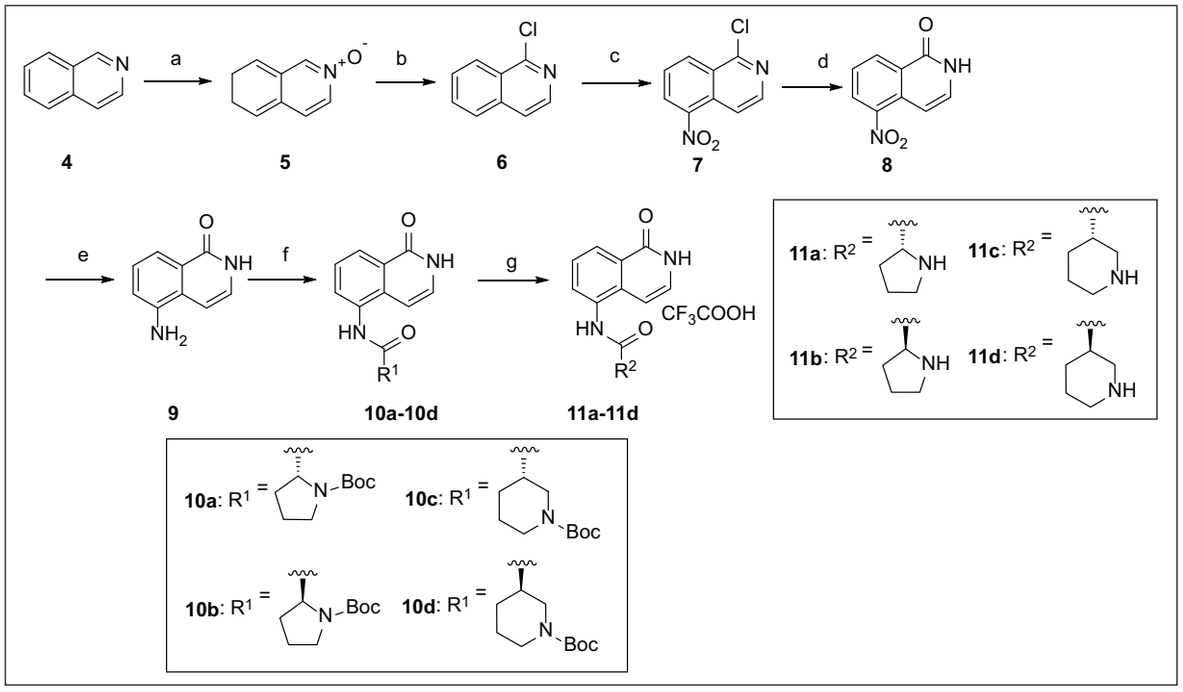

Scheme 1: Reagents and conditions: (a) *m*-CPBA, DCM, rt; (b) $POCl_3$, $CHCl_3$, reflux; (c) 70% HNO_3, H_2SO_4, 0 °C; (d) AcOH, 100 °C; (e) H_2, Pd/C, EtOH, aq HCl, rt; (f) R_1COCl, pyridine, rt; (g) TFA, DCM, rt.

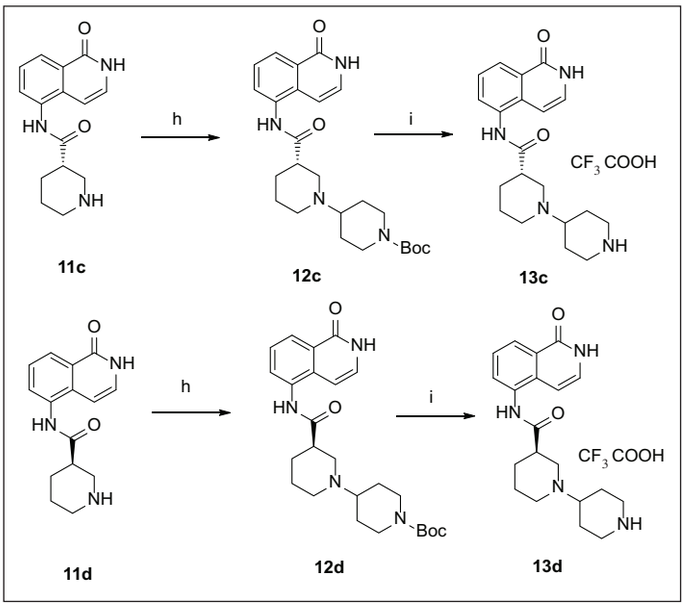

Scheme 2: Reagents and conditions: (h) *N*-Boc-4-piperidone, $NaBH(OAc)_3$, DIEA, THF, rt; (i) TFA, DCM, rt.

2. Investigations, results and discussion

2.1. Chemistry

The synthesis route of the target compounds (**10a–10d**, **11a–11d**, **12c–12d**, and **13c–13d**) is visualized in Schemes 1 and 2, according to previously published studies (Sunderland et al. 2011; Trujillo et al. 2007). Isoquinoline (**4**) was allowed to react with 3-chlorobenzoperoxoic acid in an ice bath to produce isoquinoline 2-oxide (**5**), which was then allowed to react with phosphoryl trichloride under reflux in chloroform to produce 1-chloroisoquinoline (**6**). In the presence of 70% nitric acid and concentrated sulfuric acid, compound **6** was transformed to 1-chloro-5-nitroisoquinoline (**7**), which was then hydrolyzed in the presence of acetic acid to produce compound **8**. Following treatment with 10% palladium on carbon, compound **8** was hydrogenated to produce compound **9** which was the key intermediate for preparing various target molecules. Target molecules **10a–10d** were prepared at moderate to high yields by acylation of compound **9** with the corresponding aminoacyl chloride in pyridine. The *tert*-butoxycarbonyl protecting (Boc) group was removed from compounds **10a–10d** to produce compounds **11a–11d** in the presence of trifluoroacetic acid. Compounds **12c** and **12d** were synthesized from compounds **11c** and **11d** through reductive alkylation with *N*-Boc-4-piperidone, and the Boc group of compounds **12c** and **12d** was generated from compounds **13c** and **13d** (Sunderland et al. 2011; Trujillo et al. 2007).

2.2. Inhibition of TNKS1/2 activity

Inhibition of TNKS1/2 and PARP-1 enzymes by the target compounds **10a–10d**, **11a–11d**, **12c–12d**, and **13c–13d** was evaluated, and cellular activity of these compounds was examined using a human colorectal cancer DLD-1 cell line SuperTopFlash (STF) assay. The respective results are shown as IC_{50} values (Table 1).

Even though the study of Woon et al. (2013) showed that compound **9** inhibits PARP-1 and -2, our results suggest little or no inhibition of PARP-1 by the tested compounds; therefore, we mainly focused on inhibition of TNKS1/2 enzymes and Wnt signaling in DLD-1 cells using a Wnt-responsive STF assay. XAV-939 was used as a positive control, and the respective IC_{50} values are shown in Table 1. In target compounds **11a–11d**, different *α*- or *β*-amino acids were introduced at the C-5 position amino group of 5-aminoisoquinolin-1(2*H*)-one through amide bonds. When *D*-proline was introduced, the IC_{50} values of compound **11a** against TNKS1 and TNKS2 were 0.011 and 0.033 μM, respectively, and in the DLD-1 STF assay, compound **11a** showed inhibitory effects at an IC_{50} of 0.189 μM. The *L*-proline-derivative compound **11b** showed four-fold less TNKS1 inhibition than compound **11a** but two-fold stronger inhibition of TNKS2, with IC_{50} values of 0.046 and 0.018 μM, respectively. Out of all tested compounds, compound **11c**, which contained an (*S*)-piperidine-3-formyl moiety, showed the strongest inhibition effects in both enzymatic assays (TNKS1/2 inhibition at an IC_{50} of 0.009 and 0.003 μM, respectively) and in the STF assay (IC_{50} 0.029 μM). This suggests that the size of the substituent ring or the position of the nitrogen may be key characteristics for potential future activity improvements. Compound **11d** was less potent than its isomer **11c**, with IC_{50} values of 0.022 μM (TNKS1), 0.027 μM (TNKS2), and 0.041 μM (STF). All Boc-protected derivatives (compounds **10a**–**10d**) showed substantially decreased potency, compared to their counterparts compounds **11a–11d**, suggesting that the large hydrophobic groups bound to the nitrogen atom may reduce binding affinity, and that *N*-Boc compounds are, in contrast to the free amines, not protonated at physiological pH conditions. Further introduction of a piperidine ring at the basic nitrogen atom of compounds **11c** and **11d** resulted in 3- to 28-fold decreased inhibition of TNKS1/2, indicating that a piperidine ring on the basic nitrogen atom of compounds **11c** and **11d** was not favorable, presumably due to steric hindrance. The activities of Boc-protected derivatives **12c** and **12d** were substantially decreased, which was consistent with the results obtained from compounds **11a–11d**.

Table 1: Chemical structures and inhibitory activities of compounds 10a–10d, 11a–11d, 12c–12d and 13c–13d

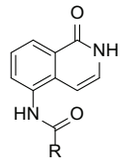

Compd.	R	TNKS1 IC^{50b}/μM	TNKS2 IC^{50b}/μM	PARP-1 IC^{50b}/μM	DLD-1 STF IC^{50c}/μM
XAV939[a]	-	0.023	0.008	0.101	0.094
10a	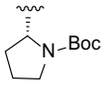	>10	0.865	>10	3.102
10b	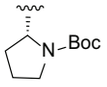	0.329	0.147	>10	1.096
10c	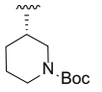	0.414	0.076	>10	0.901
10d	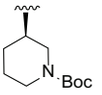	>10	0.514	>10	3.562
11a		0.011	0.033	8.276	0.189
11b		0.046	0.018	4.203	0.414
11c		0.009	0.003	>10	0.029
11d		0.022	0.027	>10	0.041
12c	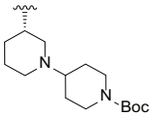	>10	1.589	>10	>10
12d	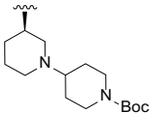	>10	>10	>10	>10
13c	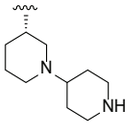	0.028	0.025	>10	0.527
13d	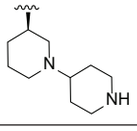	0.089	0.771	>10	1.392

a. XAV939 was used as a positive control.
b. Concentration for 50% inhibition in TNKS 1/2 or PARP-1 enzyme assay (IC_{50}).
c. Concentration for 50% inhibition in DLD-1 STF assay (IC_{50}).

2.3. Predicted binding modes

To investigate binding modes of the designed compounds, compound **11c**, which was highly potent in both enzymatic and

cellular assays, was docked to the co-crystal structure of 3-(4-chlorophenyl)-5-methyl-1,2-dihydroisoquinolin-1-one (**14**) in TNKS2 (PDB code 4UVV), which may be of interest for further structural modifications (Paine et al. 2015). As predicted, isoquinoline-1(2*H*)-one, acting as an aromatic hydrophobic skeleton, showed π-π stacking interactions with Tyr1071. The NH group in the 2-position and the CO group in the 1-position acted as hydrogen bond donor and hydrogen bond acceptor, respectively, and formed hydrogen bonds with Ser1068 and Gly1032 in the nicotinamide binding cavity, which were assumed to be the driving forces of improved binding affinity as they were frequently targeted by known TNKS inhibitors (Fig. 2B). The piperidine ring was situated in a spacious subpocket and extended to a solvent-exposed surface, which was not consistent with the characteristics of compound **14** (Fig. 2C). In addition, a hydrogen bond between the nitrogen atom of the piperidine ring and Glu1138 was observed, which was not observed in known TNKS inhibitors. Therefore, modifications of the piperidine ring may be of interest for further improving the binding affinity and drug characteristics of this series of TNKS inhibitors.

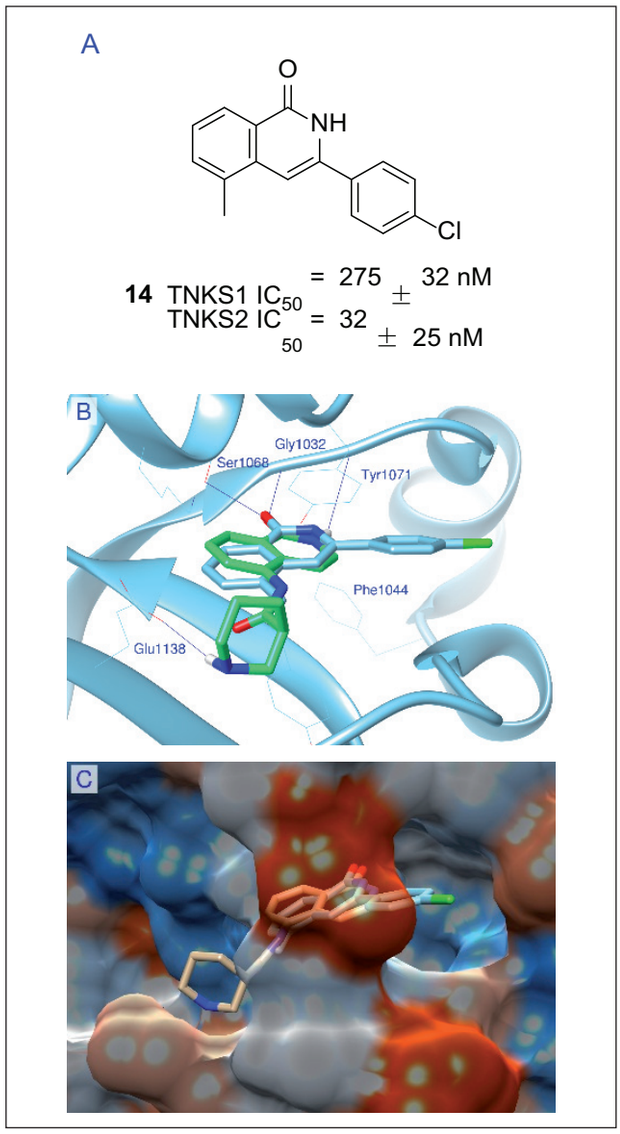

Fig. 2: (A) Molecular structure of compound **14**; (B) CDOCKER-modeled binding mode of compound **11c** (green coloration indicates carbon atoms). Binding orientation and interactions of compound **11c** in comparison with that of compound **14** (purple coloration indicates carbon atoms) in the cocrystal structure (PDB code 4UVV); H-bonding interactions are indicated by blue lines; (C) molecular structure of compound **11c** at the binding site of TNKS2 (PBD code 4UVV). Molecular structures were visualized using UCSF Chimera 1.14(Pettersen et al. 2004).

2.4. Conclusion

A series of novel isoquinolin-1(2*H*)-one derivatives was designed and synthesized. Structure-activity relationship studies demonstrated that *α*- or *β*-amino acids are favorable structural fragments in this series of TNKS inhibitors because most compounds containing these subunits demonstrated inhibitory activities with single- or double-digit nanomolar IC_{50} values. Compound **11c** showed strong inhibition in TNKS1/2 and DLD-1 STF assays, thus it may be used as a new structural template for further optimization and exploration of novel TNKS inhibitors.

3. Experimental

3.1. Chemistry

3.1.1. General

Melting points were measured on a Yanaco micro melting point apparatus and are uncorrected. Optical rotations were measured on a JASCO P-2000 polarimeter. ^{1}H NMR (300 MHz or 400 MHz) on a Varian Mercury 300 or 400 spectrometer was recorded in DMSO-d_6, acetone-d_6 or $CDCl_3$. Chemical shifts are reported in d (ppm) units relative to the internal standard tetramethylsilane (TMS). High resolution mass spectra (HRMS) were obtained on an Agilent Technologies LC/MSD TOF spectrometer. Purity of all final compounds were established by LC–HRMS analytical techniques. All compounds were found to be >95% pure by LC–HRMS analysis. All chemicals and solvents used were of reagent grade without purified or dried before use. All the reactions were monitored by thin-layer chromatography (TLC) on pre-coated silica gel G plates at 254 nm under a UV lamp. Column chromatography separations were performed with silica gel (200–300 mesh).

*3.1.2. 5 Aminoisoquinolin-1-one hydrochloride (**9**)*

Compound **9** was obtained following published procedures (Sunderland et al. 2011; Trujillo et al. 2007).

*3.1.3. tert-Butyl (R)-2-((1-oxo-1,2-dihydroisoquinolin-5-yl)carbamoyl) pyrrolidine-1-carboxylate (**10a**)*

tert-Butyl (*R*)-2-(chlorocarbonyl)pyrrolidine-1-carboxylate (326 mg, 1.40 mmol) was added to **9** (250 mg, 1.27 mmol) in pyridine (3 mL), the mixture was then stirred at room temporature overnight. Pyridine was then removed under reduced pressure, ethyl ether (3 mL) was then added to the residue. After filtration and dried under vacuum condition, compound **10a** was obtained as white solid without further purification (312 mg, 68.8%); m.p.132-134 °C; $[\alpha]^D_{20}$ +94.0 (*c* 1.05, CH_3Cl); ^{1}H NMR (300 MHz, $CDCl_3$) δ (ppm): 11.39 (1H, s), 9.78 (1H, m), 8.37 (1H, m), 8.22 (1H, d, *J* = 7.5 Hz), 7.50 (1H, t, *J* = 7.8 Hz), 7.20 (1H, d, *J* = 6.0 Hz), 6.88 (1H, m), 4.59 (1H, m), 3.52-3.44 (2H, m), 2.63 (1H, m), 1.99 (3H, m), 1.54 (9H, s) ; HR-MS (ESI): *m/z*, calcd. for $C_{19}H_{24}N_3O_4$ 358.1761 $[M+H]^+$, found: 358.1758.

*3.1.4. tert-Butyl (S)-2-((1-oxo-1,2-dihydroisoquinolin-5-yl)carbamoyl) pyrrolidine-1-carboxylate (**10b**)*

Following the preparation protocol of producing **10a**, starting from **9** (250 mg, 1.27 mmol) and *tert*-butyl (*S*)-2-(chlorocarbonyl)pyrrolidine-1-carboxylate (326 mg, 1.40 mmol), the title compound **10b** was obtained as white solid (323 mg, 71.2%); m.p.116-118 °C; $[\alpha]^D_{20}$ -92.1 (*c* 1.10, CH_3Cl); ^{1}H NMR (300 MHz, $CDCl_3$) δ (ppm): 11.43 (1H, s), 9.76 (1H, brs), 8.35 (1H, m), 8.22 (1H, d, *J* = 7.5 Hz), 7.49 (1H, t, *J* = 7.8 Hz), 7.19 (1H, d, *J* = 5.4 Hz), 6.86 (1H, m), 4.59 (1H, m), 3.47 (2H, m), 2.62 (1H, m), 1.74-1.99 (3H, m), 1.54 (9H, s); HR-MS (ESI): *m/z*, calcd. for $C_{19}H_{24}N_3O_4$ 358.1761 $[M+H]^+$, found: 358.1760.

*3.1.5. tert-Butyl (S)-3-((1-oxo-1,2-dihydroisoquinolin-5-yl)carbamoyl) piperidine-1-carboxylate (**10c**)*

Following the preparation protocol of producing **10a**, starting from **9** (100 mg, 0.51 mmol) and *tert*-butyl (*S*)-3-(chlorocarbonyl)piperidine-1-carboxylate (139 mg, 0.56 mmol), the title compound **10c** was obtained as white solid (156 mg, 82.4%); m.p.246-248 °C; $[\alpha]^D_{20}$ +21.5 (*c* 0.87, CH_3Cl); ^{1}H NMR (400 MHz, DMSO-d_6) δ (ppm): 11.33 (1H, s), 9.86 (1H, s), 8.04 (1H, d, *J* = 7.6 Hz), 7.79 (1H, d, *J* = 6.4 Hz), 7.44 (1H, t, *J* = 7.6 Hz), 7.20 (1H, m), 6.59 (1H, d, *J* = 6.8 Hz), 3.87-4.08 (2H, m), 2.64-2.90 (3H, m), 2.00-2.04 (1H, m), 1.57-1.74 (2H, m), 1.25-1.42 (10H, m); HR-MS (ESI): *m/z*, calcd. for $C_{19}H_{24}N_3O_4$ 372.1923 $[M+H]^+$, found: 372.1925.

*3.1.6. tert-Butyl (R)-3-((1-oxo-1,2-dihydroisoquinolin-5-yl)carbamoyl) piperidine-1-carboxylate (**10d**)*

Following the preparation protocol of producing **10a**, starting from **9** (100 mg, 0.51 mmol) and *tert*-butyl (*R*)-3-(chlorocarbonyl)piperidine-1-carboxylate (139 mg, 0.56 mmol), the title compound **10d** was obtained as white solid (133 mg, 70.2%); m.p.246-247 °C; $[\alpha]^D_{20}$ -22.9 (*c* 0.94, CH_3Cl); ^{1}H NMR (400 MHz, DMSO-d_6) δ (ppm): 11.47 (1H, s), 9.88 (1H, s), 8.07 (1H, d, *J* = 7.6 Hz), 7.78 (1H, d, *J* = 6.4 Hz), 7.45 (1H, t, *J* = 7.6 Hz), 7.20 (1H, m), 6.60 (1H, d, *J* = 6.8 Hz), 3.87-4.07 (2H,

m), 2.62-2.90 (3H, m), 2.01-2.05 (1H, m), 1.58-1.76 (2H, m), 1.30-1.43 (10H, m); HR-MS (ESI): *m/z*, calcd. for $C_{19}H_{24}N_3O_4$ 372.1923 $[M+H]^+$, found: 372.1927.

*3.1.7. (R)-N-(1-Oxo-1,2-dihydroisoquinolin-5-yl)pyrrolidine-2-carboxamide 2,2,2-trifluoroacetate (**11a**)*

To a stirred solution of **10a** (50 mg, 0.14 mmol) in DCM (2 mL) was added TFA (2 mL) dropwise, the reaction mixture was then allowed to stir at room temperature overnight. DCM and excessive TFA was then removed under reduced pressure, ethyl ether (2 mL) was then added to the residue. After filtration and dried under vacuum condition, compound **11a** was obtained as white solid without further purification (45 mg, 86.6%); m.p.178-180 °C; $[\alpha]^D_{20}$ +55.8 (*c* 1.00, CH_3Cl); ^1H NMR (400 MHz, DMSO-d_6) δ (ppm): 11.42 (1H, s), 10.44 (1H, s), 9.49 (1H, brs), 8.71 (1H, brs), 8.11 (1H, d, *J* = 7.6 Hz), 7.83 (1H, d, *J* = 7.2 Hz), 7.50 (1H, t, *J* = 6.8 Hz), 7.26 (1H, m), 6.61 (1H, d, *J* = 6.4 Hz), 4.53 (1H, m), 3.29 (2H, m), 1.98-2.10 (4H, m); HR-MS (ESI): *m/z*, calcd. for $C_{19}H_{24}N_3O_4$ 258.1243 $[M+H]^+$, found: 258.1241.

*3.1.8. (S)-N-(1-Oxo-1,2-dihydroisoquinolin-5-yl)pyrrolidine-2-carboxamide 2,2,2-trifluoroacetate (**11b**)*

Following the preparation protocol of producing **11a**, starting from **10b** (45 mg, 0.12 mmol), the title compound **11b** was obtained as white solid (40 mg, 85.6%); m.p.141-143 °C; $[\alpha]^D_{20}$ -55.1 (*c* 1.09, CH_3Cl); ^1H NMR (300 MHz, DMSO-d_6) δ (ppm): 11.44 (1H, s), 10.60 (1H, s), 9.86 (1H, brs), 8.70 (1H, brs), 8.10 (1H, d, *J* = 7.8 Hz), 7.83 (1H, d, *J* = 7.5 Hz), 7.50 (1H, t, *J* = 7.5 Hz), 7.23-7.26 (1H, m), 6.66 (1H, d, *J* = 6.9 Hz), 4.57 (1H, m), 3.28 (2H, m), 1.95-2.09 (3H, m); HR-MS (ESI): *m/z*, calcd. for $C_{19}H_{24}N_3O_4$ 258.1243 $[M+H]^+$, found: 358.1244.

*3.1.9. (S)-N-(1-Oxo-1,2-dihydroisoquinolin-5-yl)piperidine-3-carboxamide 2,2,2-trifluoroacetate (**11c**)*

Following the preparation protocol of producing **11a**, starting from **10c** (70 mg, 0.19 mmol), the title compound **11c** was obtained as white solid (50 mg, 68.8 %); m.p.137-139 °C; $[\alpha]^D_{20}$ +8.5 (*c* 1.17, CH_3Cl); ^1H NMR (400 MHz, DMSO-d_6) δ (ppm): 11.37 (1H, s), 10.07 (1H, s), 8.72-8.77 (2H, m), 8.07 (1H, d, *J* = 8.0 Hz), 7.78 (1H, d, *J* = 7.6 Hz), 7.46 (1H, t, *J* = 7.6 Hz), 7.22 (1H, t, *J* = 6.4 Hz), 6.59 (1H, d, *J* = 7.2 Hz), 3.37-3.40 (1H, m), 2.95-3.24 (4H, m), 2.14 (1H, m), 1.87 (1H, m), 1.70-1.78 (2H, m); HR-MS (ESI): *m/z*, calcd. for $C_{19}H_{24}N_3O_4$ 272.1399 $[M+H]^+$, found: 272.1402.

*3.1.10. (R)-N-(1-Oxo-1,2-dihydroisoquinolin-5-yl)piperidine-3-carboxamide 2,2,2-trifluoroacetate (**11d**)*

Following the preparation protocol of producing **11a**, starting from **10d** (70 mg, 0.19 mmol), the title compound **11d** was obtained as white solid (65 mg, 89.4 %); m.p.138-139 °C; $[\alpha]^D_{20}$ -8.2 (*c* 0.98, CH_3Cl); ^1H NMR (400 MHz, DMSO-d_6) δ (ppm): 11.47 (1H, s), 10.06 (1H, s), 8.72-8.75 (2H, m), 8.05 (1H, d, *J* = 8.0 Hz), 7.77 (1H, d, *J* = 7.6 Hz), 7.45 (1H, t, *J* = 7.6 Hz), 7.22 (1H, t, *J* = 6.4 Hz), 6.60 (1H, d, *J* = 7.2 Hz), 3.35-3.41 (1H, m), 2.96-3.23 (4H, m), 2.15 (1H, m), 1.88 (1H, m), 1.70-1.78 (2H, m); HR-MS (ESI): *m/z*, calcd. for $C_{19}H_{24}N_3O_4$ 272.1399 $[M+H]^+$, found: 272.1400.

*3.1.11. tert-Butyl (S)-3-((1-oxo-1,2-dihydroisoquinolin-5-yl)carbamoyl)-[1,4'-bipiperidine]-1'-carboxylate (**12c**)*

To a suspension of **11c** (160 mg, 0.42 mmol) and *tert*-butyl 4-oxopiperidine-1-carboxylate (250 mg, 1.26 mmol) at 0°C in THF (20 mL), DIEA (0.21 ml, 1.26 mmol) were added with caution. The mixture was heated to room temperature and stirred for 8 h, then $NaBH(OAc)_3$ (268 mg, 1.26 mmol) was added to the mixture and stired at room temperature for 48 h. After filtration and concentration, the crude product was obtained and purified with column chromatography on silica gel to afford compound **12c** as white solid (115 mg, 46.4%); m.p. 131-133 °C; $[\alpha]^D_{20}$ +65.3 (*c* 0.81, CH_3Cl); ^1H NMR (300 MHz, $CDCl_3$) δ (ppm): 11.15 (1H, s), 8.15-8.18 (2H, m), 7.41-7.48 (1H, m), 7.13 (1H, m), 6.59-6.62 (1H, m), 4.22 (2H, m), 2.69-3.79 (8H, m), 1.58-1.91 (8H, m), 1.44 (9H, s) ; HR-MS (ESI): *m/z*, calcd. for $C_{25}H_{35}N_4O_4$ 455.2653 $[M+H]^+$, found: 455.2669.

*3.1.12. tert-Butyl (R)-3-((1-oxo-1,2-dihydroisoquinolin-5-yl)carbamoyl)-[1,4'-bipiperidine]-1'-carboxylate (**12d**)*

Following the preparation protocol of producing **12c**, starting from **11d** (160 mg, 0.42 mmol) and *tert*-butyl 4-oxopiperidine-1-carboxylate (250 mg, 1.26 mmol) , the title compound **12d** was obtained as white solid (156 mg, 62.9%); m.p. 131-133 °C; $[\alpha]^D_{20}$ -66.1 (*c* 0.80, CH_3Cl); ^1H NMR (300 MHz, $CDCl_3$) δ (ppm): 11.17 (1H, s), 8.16-8.19 (2H, m), 7.43-7.49 (1H, m), 7.14 (1H, m), 6.56-6.61 (1H, m), 4.25-4.28 (2H, m), 2.74-3.79 (8H, m), 1.87 (8H, m), 1.43 (9H, s); HR-MS (ESI): *m/z*, calcd. for $C_{25}H_{35}N_4O_4$ 455.2653 $[M+H]^+$, found: 455.2666.

*3.1.13. (S)-N-(1-Oxo-1,2-dihydroisoquinolin-5-yl)-[1,4'-bipiperidine]-3-carboxamide 2,2,2-trifluoroacetate (**13c**)*

Following the preparation protocol of producing **11a**, starting from **12c** (20 mg, 0.04 mmol), the title compound **13c** was obtained as white solid (18 mg, 87.3%); m.p.160-162 °C; $[\alpha]^D_{20}$ +39.4 (*c* 0.75, CH_3Cl); ^1H NMR (400 MHz, DMSO-d_6) δ (ppm): 11.37 (1H, s), 10.10 (1H, s), 8.90 (1H, brs), 8.56 (1H, brs), 8.05-8.09 (1H, m), 7.74 (1H, m), 7.47 (1H, m), 7.21 (1H, m), 6.57-6.60 (1H, m), 2.96-3.64 (9H, m), 1.53-2.22 (8H, m); HR-MS (ESI): *m/z*, calcd. for $C_{19}H_{24}N_3O_4$ 355.2134 $[M+H]^+$, found: 355.2133.

*3.1.14. (R)-N-(1-Oxo-1,2-dihydroisoquinolin-5-yl)-[1,4'-bipiperidine]-3-carboxamide 2,2,2-trifluoroacetate (**13d**)*

Following the preparation protocol of producing **11a**, starting from **12d** (100 mg, 0.20 mmol), the title compound **13d** was obtained as white solid (96 mg, 93.1%); m.p. 161-162 °C; $[\alpha]^D_{20}$ -39.0 (*c* 0.77, CH_3Cl); ^1H NMR (400 MHz, DMSO-d_6) δ (ppm): 11.28 (1H, s), 10.22 (1H, s), 8.94 (1H, brs), 8.56 (1H, brs), 8.07-8.11 (1H, m), 7.74 (1H, m), 7.45 (1H, m), 7.21 (1H, m), 6.55-6.61 (1H, m), 2.88-3.75 (9H, m), 1.46-2.13 (8H, m); HR-MS (ESI): *m/z*, calcd. for $C_{19}H_{24}N_3O_4$ 355.2134 $[M+H]^+$, found: 355.2136.

3.2. TNKS1/2 and PARP-1 assays

The ability of compounds to inhibit TNKS1/2 and PARP-1 enzyme activity was tested using the ELISA method as described (Hua et al. 2013; Putt and Hergenrother 2004; Zhou et al. 2018). IC_{50} values were calculated using GraphPad Prism 5 software.

3.3. DLD-1 STF assay

DLD-1 colorectal cells engineered with an 8× TCF promoter-driven firefly (FF) luciferase gene (wnt reporter) along with an EF1a promoter-driven Renilla (RN) luciferase gene (control reporter) were used to measure the potency of tankyrase compounds in the context of the constitutively activated wnt pathway due to mutated APC in colorectal cancer cells. The engineered DLD-1 cells were plated at a density of 10000 cells/ well in black, clear-bottom, 96-well View plates in normal growth medium (RPMI with 10% FBS with no antibiotics). Tankyrase inhibitors were transferred to cells from a 3-fold serially diluted compound plate. A 10-point dilution series was tested starting at 10 µM. The plates were incubated at 37 °C for 48 h. The Dual-Glo reagents (Promega) were added as directed by the manufacturer to assess the firefly (FF) and Renilla (RN) luciferase activity. Luciferase activity was measured using the EnVision multilabel plate reader.

3.4. Molecular docking

The CDOCKER protocol in Discovery Studio 2016 (Accelrys Software Inc., San Diego, CA) was used in this study to investigate the binding mode of compound **11c** in the crystal structure TNKS2. CDOCKER uses molecular dynamics (MD) with CHARMm force field scheme to dock ligands into binding sites of target proteins. Water molecules in the protein were removed and the protein was prepared by adding hydrogen and correcting the incomplete residues using Clean Protein tool of Discovery Studio, then the protein was refined with CHARMm force field. The binding site was constructed within 8.0 Å with **14** set as the center. Compound **11c** was built and minimized using Prepare Ligands tool of Discovery Studio and refined with CHARMm force field. Docking of compound **11c** into TNKS2 with CDOCKER was done using the default parameters except that Pose Cluster Radius was defined as 0.5 Å in order to increase the diversity of docking poses. The pose with top –CDOCKER_INTERACTION_ENERGY was chosen for analyzing the binding features of compound **11c** and TNKS2.

Funding: This work was supported by the Yichang Medical and Health Research Project (A20-2-010).

Conflict of Interest: The authors declare that they have no competing interests.

References

Bregman H, Chakka N, Guzman-Perez A, Gunaydin H, Gu Y, Huang X, Berry V, Liu J, Teffera Y, Huang L, Egge B, Mullady EL, Schneider S, Andrews PS, Mishra A, Newcomb J, Serafino R, Strathdee CA, Turci SM, Wilson C, DiMauro EF (2013) Discovery of novel, induced-pocket binding oxazolidinones as potent, selective, and orally bioavailable tankyrase inhibitors. J Med Chem 56: 4320–4342.

Croy HE, Fuller CN, Giannotti J, Robinson P, Foley AV, Yamulla RJ, Cosgriff S, Greaves BD, von Kleeck RA, An HH, Powers CM, Tran JK, Tocker AM, Jacob KD, Davis BK, Roberts DM (2016) The poly(ADP-ribose) polymerase enzyme tankyrase antagonizes activity of the beta-catenin destruction complex through ADP-ribosylation of Axin and APC2. J Biol Chem 291: 12747–12760.

Ferri M, Liscio P, Carotti A, Asciutti S, Sardella R, Macchiarulo A, Camaioni E (2017) Targeting Wnt-driven cancers: Discovery of novel tankyrase inhibitors. Eur J Med Chem 142: 506–522.

Haikarainen T, Narwal M, Joensuu P, Lehtiö L (2013a) Evaluation and structural basis for the inhibition of tankyrases by PARP Inhibitors. ACS Med Chem Lett 5: 18–22.

Haikarainen T, Venkannagari H, Narwal M, Obaji E, Lee HW, Nkizinkiko Y, Lehtio L (2013b) Structural basis and selectivity of tankyrase inhibition by a Wnt signaling inhibitor WIKI4. PLoS One 8: e65404.

Hua Z, Bregman H, Buchanan JL, Chakka N, Guzman-Perez A, Gunaydin H, Huang X, Gu Y, Berry V, Liu J, Teffera Y, Huang L, Egge B, Emkey R, Mullady EL, Schneider S, Andrews PS, Acquaviva L, Dovey J, Mishra A, Newcomb J, Saffran D, Serafino R, Strathdee CA, Turci SM, Stanton M, Wilson C, Dimauro EF (2013) Development of novel dual binders as potent, selective, and orally bioavailable tankyrase inhibitors. J Med Chem 56: 10003–10015.

Narwal M, Venkannagari H, Lehtio L (2012) Structural basis of selective inhibition of human tankyrases. J Med Chem 55: 1360–1367.

Paine HA, Nathubhai A, Woon EC, Sunderland PT, Wood PJ, Mahon MF, Lloyd MD, Thompson AS, Haikarainen T, Narwal M, Lehtio L, Threadgill MD (2015) Exploration of the nicotinamide-binding site of the tankyrases, identifying 3-arylisoquinolin-1-ones as potent and selective inhibitors in vitro. Bioorg Med Chem 23: 5891–5908.

Pettersen EF, Goddard TD, Huang CC, Couch GS, Greenblatt DM, Meng EC, Ferrin TE (2004) UCSF Chimera?A visualization system for exploratory research and analysis. J Comput Chem 25: 1605–1612.

Putt KS, Hergenrother PJ (2004) An enzymatic assay for poly(ADP-ribose) polymerase-1 (PARP-1) via the chemical quantitation of NAD^+: application to the high-throughput screening of small molecules as potential inhibitors. Anal Biochem 326: 78–86.

Riffell JL, Lord CJ, Ashworth A (2012) Tankyrase-targeted therapeutics: expanding opportunities in the PARP family. Nat Rev Drug Discov 11: 923–936.

Seimiya H, Muramatsu Y, Ohishi T, Tsuruo T (2005) Tankyrase 1 as a target for telomere-directed molecular cancer therapeutics. Cancer Cell 7: 25–37.

Shultz MD, Cheung AK, Kirby CA, Firestone B, Fan J, Chen CH, Chen Z, Chin DN, Dipietro L, Fazal A, Feng Y, Fortin PD, Gould T, Lagu B, Lei H, Lenoir F, Majumdar D, Ochala E, Palermo MG, Pham L, Pu M, Smith T, Stams T, Tomlinson RC, Toure BB, Visser M, Wang RM, Waters NJ, Shao W (2013) Identification of NVP-TNKS656: the use of structure-efficiency relationships to generate a highly potent, selective, and orally active tankyrase inhibitor. J Med Chem 56: 6495–6511.

Sonnenblick A, de Azambuja E, Azim HA, Jr., Piccart M (2015) An update on PARP inhibitors--moving to the adjuvant setting. Nat Rev Clin Oncol 12: 27–41.

Sunderland PT, Woon ECY, Dhami A, Bergin AB, Mahon MF, Wood PJ, Jones LA, Tully SR, Lloyd MD, Thompson AS, Javaid H, Martin NMB, Threadgill MD (2011) 5-Benzamidoisoquinolin-1-ones and 5-(ω-Carboxyalkyl)isoquinolin-1-ones as isoform-selective inhibitors of poly(ADP-ribose) polymerase 2 (PARP-2). J Med Chem 54: 2049–2059.

Trujillo JI, Huang HC, Neumann WL, Mahoney MW, Long S, Huang W, Garland DJ, Kusturin C, Abbas Z, South MS, Reitz DB (2007) Design, synthesis, and biological evaluation of pyrazinones containing novel P1 needles as inhibitors of TF/VIIa. Bioorg Med Chem Lett 17: 4568–4574.

Woon ECY, Sunderland PT, Paine HA, Lloyd MD, Thompson AS, Threadgill MD (2013) One-pot tandem Hurtley–retro-Claisen–cyclisation reactions in the synthesis of 3-substituted analogues of 5-aminoisoquinolin-1-one (5-AIQ), a water-soluble inhibitor of PARPs. Biorg Med Chem 21: 5218–5227.

Yao H, Ji M, Zhu Z, Zhou J, Cao R, Chen X, Xu B (2015) Discovery of 1-substituted benzyl-quinazoline-2,4(1*H*,3*H*)-dione derivatives as novel poly(ADP-ribose)polymerase-1 inhibitors. Biorg Med Chem 23: 681–693.

Yao H, Zhu Z, Ji M, Chen X, Xu B (2014) Design, synthesis and biological evaluation of novel para-substituted 1-benzyl-quinazoline-2, 4 (1*H*, 3*H*)-diones as human PARP-1 inhibitors. Acta Pharm Sin 49: 497–503.

Zhou J, Ji M, Yao H, Cao R, Zhao H, Wang X, Chen X, Xu B (2018) Discovery of quinazoline-2,4(1*H*,3*H*)-dione derivatives as novel PARP-1/2 inhibitors: design, synthesis and their antitumor activity. Org Biomol Chem 16: 3189–3202.